

Section 1

PROGRESS IN LASER FUSION

1.A Saturation and Power Balance in Multibeam Lasers for Laser Fusion

Introduction: Irradiation Uniformity Considerations for Laser Fusion

Successful demonstration of laser-fusion feasibility is critically dependent on the ability to drive the implosion with a very high degree of symmetry over the whole time of the target irradiation. For direct-drive laser fusion, this implies an irradiation uniformity over the entire surface of the target, which should not deviate from perfect uniformity by more than $\approx 1\%$ rms at any time.¹ Such uniformity can only be realistically achieved with a fairly large number of incident laser beams symmetrically disposed around the target.² At the same time each of these beams must have a reproducible on-target beam intensity distribution that must be the same for all beams and should also be as smooth as possible.³ (The exact definition of smoothness, including temporal variations of any microstructure in the intensity distribution, is under investigation at present and will not be discussed further in this section.) To maintain a high degree of irradiation uniformity over the entire laser-pulse duration, equal power in each of the beams is required at any time, hence the term "power balance." If all beams are power balanced then all beam energies are the same. Since experimentally it is much easier to measure laser-pulse energy than instantaneous power in each beam, energy balance has been recognized to be essential for laser fusion. Power balance is obtained as a consequence of energy balance if all beamlines are identical. However, typical high-power beamlines are not identical, the consequences of which are the subject of the present study.

The study was stimulated by recent efforts at LLE to achieve high densities in direct-drive laser-fusion experiments with neutron yields

comparable to those predicted by one-dimensional hydrodynamic code simulations.⁴ These experiments have led to an investigation of all aspects of irradiation uniformity and prompted many measurements relating input and output temporal pulse shapes, energy balance, and gains and losses in the 24 beamlines of OMEGA—a frequency-tripled Nd:glass laser system.^{5,6,7} All nonlinear effects on a laser beam along its path from oscillator to target are potential contributors to power imbalance (linear effects are easily compensated for by attenuators or simple redistribution of energy among beamlines). The primary nonlinear effects include gain saturation in the laser amplifiers and harmonic frequency conversion at the output. In the following sections these two effects will be treated separately: first, the generic problem of amplifier saturation, which affects essentially all large, efficiently designed laser systems; second, the effects of harmonic conversion, which apply only to lasers with harmonic converters at their output.

Saturation in Laser Amplifiers

Saturation in laser amplifiers is well understood⁸ and is due to energy extraction from the active medium. Trenholme⁹ has shown how Gaussian temporal pulses are distorted if a single saturated amplifier is considered, or if the main saturation effects only occur in the final laser amplifier. The distortion of more complex shaped pulses was treated for the OMEGA laser system some time ago;¹⁰ however, the situation becomes considerably more complicated if we consider modern, more efficient laser designs with many beams.¹¹ In such lasers an attempt is made to extract as much energy as possible from each amplifier stage without incurring damage or other deleterious effects. This leads to distributed saturation effects whose total temporal pulse distortion far exceeds that predicted for a saturated final amplifier only. On the other hand, the problem still maintains Trenholme's essential conclusion that the ratio of the output fluence to the saturated fluence ($F_{\text{out}}/F_{\text{sat}}$) is the most important parameter. For the case of distributed saturation, the saturation pulse distortion depends on $F_{\text{out}}/F_{\text{sat}}$ in each of the amplifier stages where this ratio exceeds a value of $F_{\text{out}}/F_{\text{sat}} \gtrsim 0.1$.

The small-signal gain G_o of an active medium is observed experimentally only if the output fluence is small compared to the saturation fluence; otherwise, the output fluence of a loss-less amplifier is given by the Frantz-Nodvik equation¹²

$$F_{\text{out}} / F_{\text{sat}} = \ell n \left\{ 1 + G_o \left[\exp (F_{\text{in}} / F_{\text{sat}} - 1) \right] \right\} , \quad (1)$$

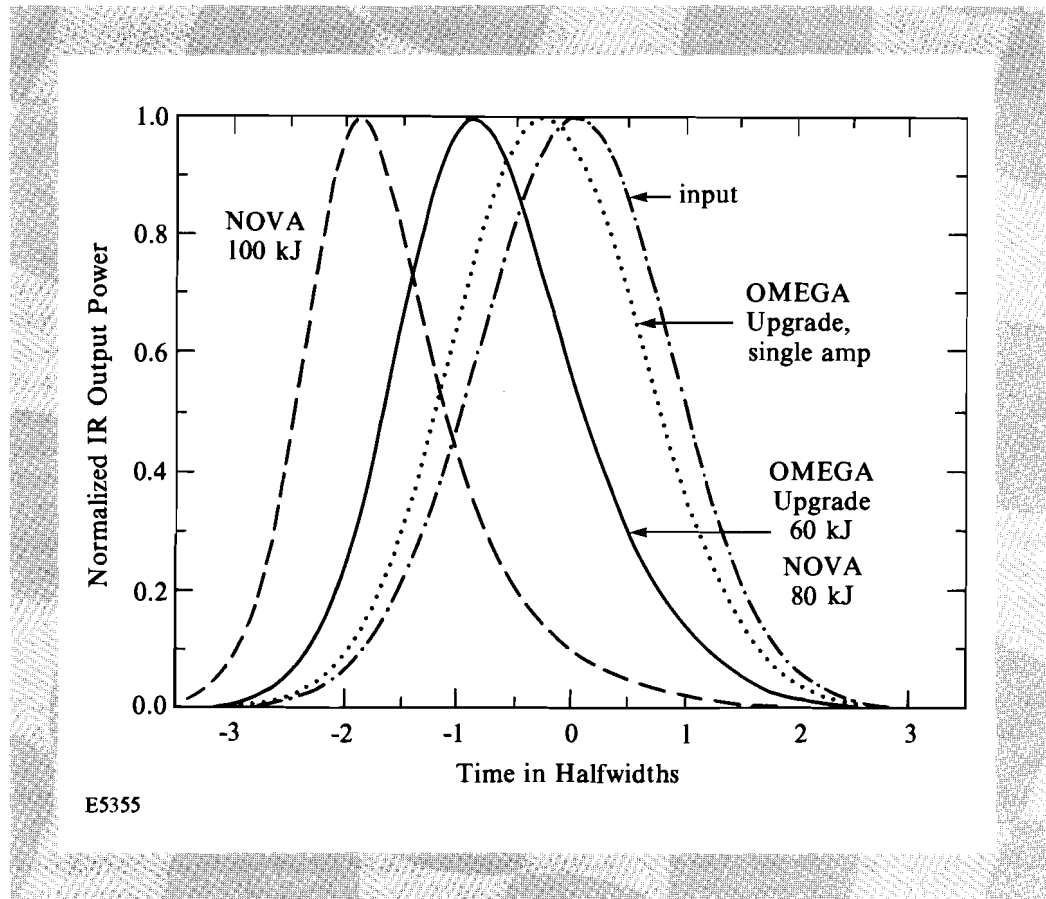
where F_{in} is the input fluence to the amplifier. The small-signal gain can also be written as $G_o = \exp(E_{\text{st}} \ell / F_{\text{sat}}) = \exp(F_{\text{st}} / F_{\text{sat}})$, where E_{st} is the stored energy in J/cm^3 , ℓ is the length of the amplifier, and F_{st} is a stored fluence in J/cm^2 , i.e., the stored energy per unit area. Since all fluences appear only as ratios relative to F_{sat} , all conclusions relating to saturated amplification are therefore generic for any laser system.

No information on temporal pulse-shape distortions can be obtained from Eq. (1). However, if we divide the incident pulse into small temporal segments and the amplifier into small spatial segments, we can propagate each temporal segment through the amplifier and follow the temporal evolution of the entire pulse as it passes through the amplifier, provided we

reduce the stored energy in each spatial segment by the energy extracted by each temporal segment as it is amplified. We have written a simple code that calculates this pulse distortion for any number of amplifiers including losses, beam expanders, and beam splitters. Within each spatial segment these calculations use the small-signal gain for this segment as the fluences per temporal interval are sufficiently small.

The most obvious manifestation of saturation distortion of Gaussian laser pulses is the shift of the pulse maxima toward earlier times as evident in Fig. 41.1. The figure shows the output pulse shape for the 60-kJ design output energy at the fundamental laser wavelength of $\lambda_L = 1.054 \mu\text{m}$ for the planned 60-beam OMEGA Upgrade Nd:glass laser, whose proposed staging diagram is shown in Fig. 41.2. For this case the output fluence just after the final amplifier is $1.25 \times F_{\text{sat}}$. The abscissa of Fig. 41.1 was chosen in terms of halfwidths of the laser pulse since the pulse distortion is independent of the actual pulse duration for 0.5-ns to 10-ns pulses,¹³ the typical range of interest for fusion lasers. The saturation distortion becomes more important as the laser is designed to be more efficient, i.e., as the output fluences in the intermediate and final amplifiers approach or exceed the saturation fluence. This is easily seen in the dotted pulse shape in Fig. 41.1, which is obtained if a hypothetical amplifier is assumed whose small-signal gain equals the combined gain of all the amplifiers in Fig. 41.2 and without intermediate losses, beam splitters, or magnifying spatial filters. Clearly the pulse distortion is much reduced in this case but such a laser would be very inefficient and cost prohibitive.

Fig. 41.1
Distortion of Gaussian input pulses in large laser chains.



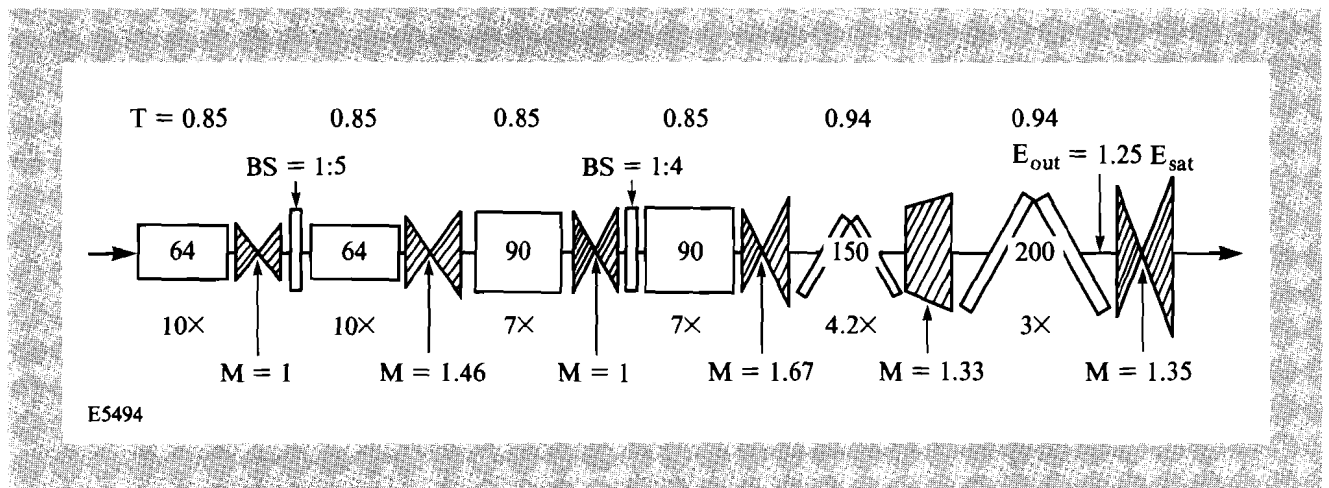


Fig. 41.2

Staging diagram for the proposed OMEGA Upgrade laser. Nominal sizes are shown inside each amplifier; small-signal gains are shown below each amplifier; typical transmission losses and beam-splitting ratios are shown above the amplifiers.

It is interesting to compare the pulse-shape distortion calculated for the OMEGA Upgrade with that expected for the NOVA laser system at the Lawrence Livermore National Laboratory.¹¹ At the 80-kJ output level the pulse-shape distortion is practically indistinguishable from that for the 60-kJ OMEGA Upgrade design (solid line in Fig. 41.1). This is surprising in light of the completely different amplifier staging for the two laser systems. However, the pulse distortion for NOVA at 100-kJ output is dramatically higher (left-most curve in Fig. 41.1); for the recently demonstrated 120-kJ output capability of NOVA the output pulse shifts practically out of the range plotted in Fig. 41.1.

Power Balance in Multibeam Laser Systems

If a large number of beams are incident on the target with the requirement of continued instantaneous near-perfect irradiation uniformity, we must have equal powers, i.e., equal pulse shapes, in all irradiating laser beams. Since laser-pulse distortion increases with laser efficiency we can expect a concomitant increase in sensitivity of the temporal pulse shapes of the various beams to small fluctuations in individual beam energies. These energies can typically be measured with an accuracy of $\leq 1\%$ and, under optimum conditions, rms beam-energy-balance values of 1% to 2% have been achieved.^{14,15} However, the corresponding peak-to-valley excursions in beam energies are typically 3 to 4 times larger. Therefore, it is important to know the consequences of such energy imbalances on the power balance between individual beams.

Figure 41.3 shows the calculated, temporally dependent power imbalance $\Delta P/P_{av}$ for pairs of beams whose energies differ by 5% and for the same laser configurations, output fluences, and output energies as shown in Fig. 41.1. We notice that the 5% beam-energy imbalance at the output of the laser chain translates into $\leq 18\%$ power imbalance at early times of the originally Gaussian laser pulse for the OMEGA Upgrade design specifications. For the 100-kJ NOVA output the power imbalance is considerably worse, while the

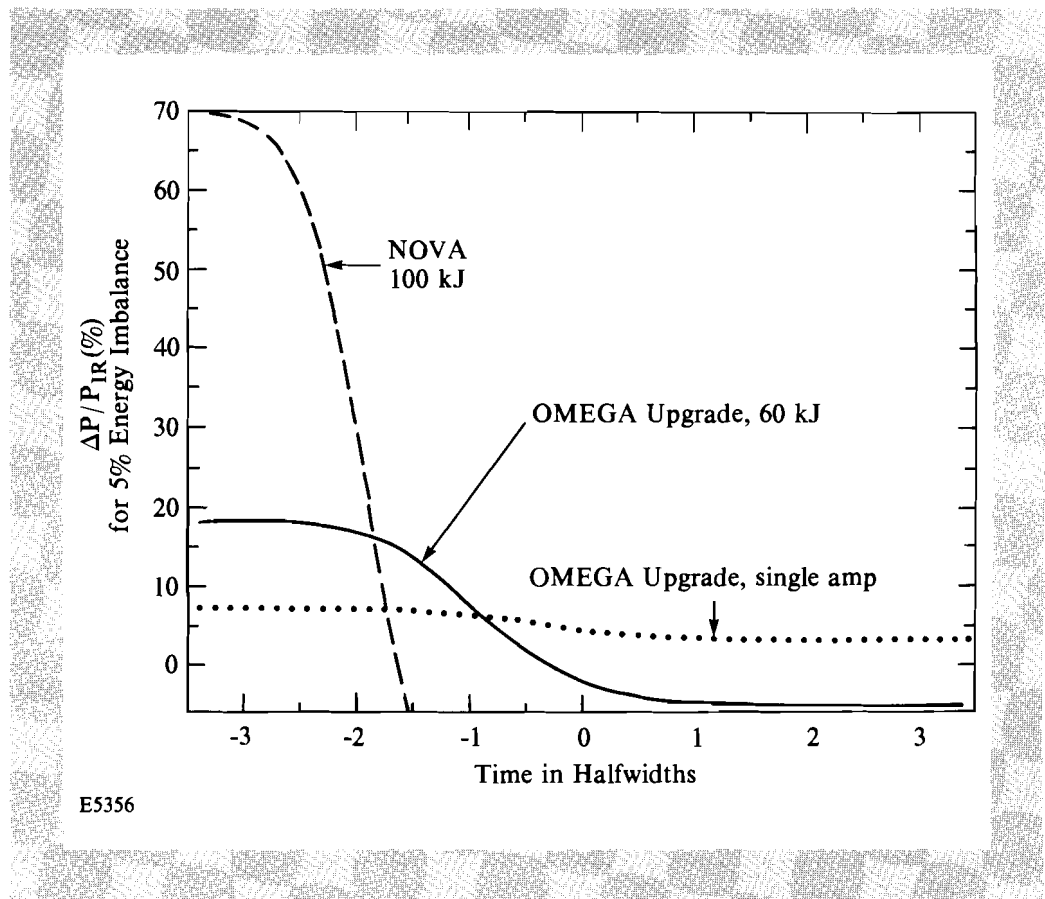


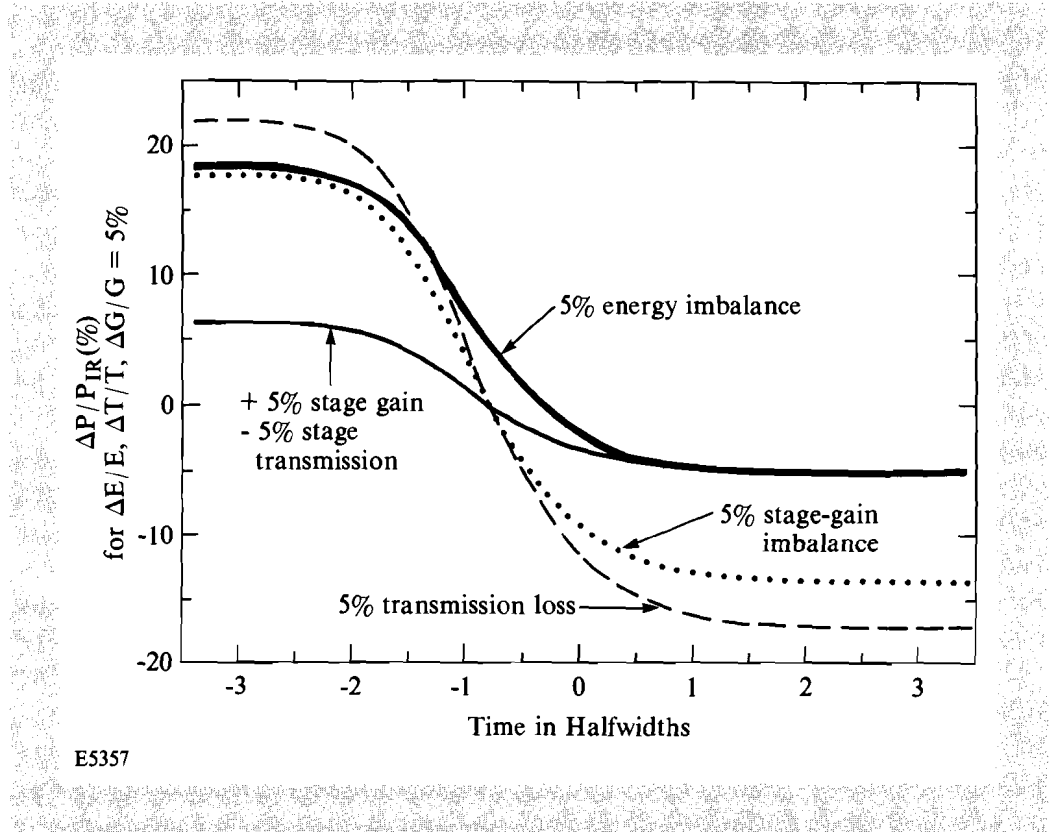
Fig. 41.3

Temporal dependence of the IR power balance between two beamlines of the proposed OMEGA Upgrade (University of Rochester) and NOVA (Lawrence Livermore National Laboratory) laser systems for two beamlines whose output energies differ by 5%.

curve for 80-kJ NOVA is indistinguishable from that for the OMEGA Upgrade at full design value. We note that at $\approx 2\%$ of the peak output power the power imbalance is still approximately 95% of its asymptotic early-time value in all cases.

The curves in Fig. 41.3 were calculated for identical gains and losses in the laser chain under the assumption that the only contributor to the energy imbalance was the input energy to the amplifier chain. This, however, is only one possible scenario leading to power imbalance due to amplifier saturation. Alternative sources for power imbalance include differing gains and/or losses along the laser chain. To assess their relative importance we assume perfect energy balance but differing gains (losses) in the two beams whose temporal power imbalance $\Delta P/P_{av}$ is to be evaluated. In addition, we can also assume compensating small-signal gains and losses in each stage such that the net small-signal gain remains unchanged. We have further assumed that any changes in gains or losses are made in the same sense (increasing or decreasing) in all stages of one beamline.

The power imbalances due to energy imbalance, gain imbalance, loss imbalance, and compensated gain-loss imbalances are shown in Fig. 41.4 for the nominal 60-kJ OMEGA Upgrade design. The abscissa of this graph represents the relative changes in the variables under consideration ($\Delta E/E$, $\Delta G/G$, etc.). A value of $\Delta G/G$ (or $\Delta T/T$) = 5% implies that the small-signal gain [or transmission = 1 - (loss)] of each amplifier stage in one of the two beams was increased by 5%. Thus, for the staging diagram of Fig. 41.2 with six amplifier stages, a 5% change in stage gain corresponds to $\approx 30\%$ change in total small-signal system gain. While this may appear to be a large gain imbalance, actual gain variations between beams in large laser systems can easily exceed such values.



E5357

Fig. 41.4

Temporal dependence of the IR power imbalance between two beamlines of the OMEGA Upgrade at nominal 60-kJ output with a Gaussian temporal pulse as shown in Fig. 41.1. The different curves relate to power imbalance due to 5% energy imbalance between the two beams (heavy solid line), 5% per stage gain imbalance (dotted line), 5% per stage loss imbalance (dashed line), and compensated 5% gain and loss balance per stage ($\Delta G/G = -\Delta T/T = 5\%$, thin solid line).

Perfect energy balance but unequal gains or losses in two different beams can lead to very pronounced power imbalance, as shown in Fig. 41.4. Significantly lower power imbalance is observed if the losses and gains are balanced in each stage such that the product of gain and transmission is constant. In other words, we may increase the gain in each stage by 5% without degrading the power balance unduly, provided we increase the

losses (decrease the transmission T) in each stage correspondingly. This result is intuitively obvious and the calculations bear this out very clearly (see the thin solid curve in Fig. 41.4).

The implications of Fig. 41.4 are several-fold: Power balance requires energy balance plus detailed gain and loss balance throughout the laser system. The exact requirements for energy, gain, and loss balance depend strongly on the detailed laser design; in particular, as the laser design becomes more efficient, i.e., as the fluence levels approach or exceed the saturation fluence, the demands on energy, gain, loss, and detailed interstage gain-loss balance become significantly more stringent and harder to meet.

Power Balance and Harmonic Conversion

Over the past ten years, laser-fusion research has shown that irradiation wavelengths of $\leq 0.5 \mu\text{m}$ are required to achieve acceptable target performance. For lasers with longer fundamental wavelengths, this requirement implies harmonic conversion of the laser output; however, the inherently nonlinear nature of harmonic frequency conversion is a source of great concern for power balance.

We now turn to the problems associated with third-harmonic conversion of 1- μm glass lasers for which the relevant third-harmonic energy-conversion curve is shown in Fig. 41.5. Also shown in this figure are the conversion curves for angle- and polarization-detuned crystals⁶ as well as experimental data obtained on the 24-beam OMEGA laser facility. The narrow cross-hatched area close to the theoretical optimum crystal performance includes the rms performance of all 24 conversion-crystal cells for over 70 OMEGA target shots. The worst-performing conversion cells for the same set of shots have conversion efficiencies that lie within the larger cross-hatched band labeled "p-v" (peak-to-valley). We note that in an rms sense all data indicate crystal-tuning capability within $\leq 50 \mu\text{rad}$, with the worst performers exceeding $100 \mu\text{rad}$ by a small amount. Since these measurements were taken, mechanical improvements have been made to the cell mounts that should further reduce these error bars; however, we have not yet collected a sufficiently large new data base to quantify the improvements.

Detuned conversion crystals rapidly lead to pulse-shape distortions and concomitant increases in power imbalance as discussed in Ref. 16. However, even perfectly tuned crystal converters significantly aggravate any IR power-balance problems incident on them (see Fig. 41.6). This figure is analogous to Fig. 41.4 but includes third-harmonic conversion for perfectly tuned crystals. Note that the 18% IR power imbalance generated by a 5% IR energy imbalance for the nominal OMEGA Upgrade output results in a $>50\%$ power imbalance at the third-harmonic output. The corresponding third-harmonic power at that time is $\approx 10^{-3}$ of the peak power, i.e., at a time when relatively little plasma surrounds the laser-fusion target and no significant thermal smoothing is expected.

Power imbalance as a result of different gains or losses in the individual amplification stages of the two beamlines also leads to much higher power

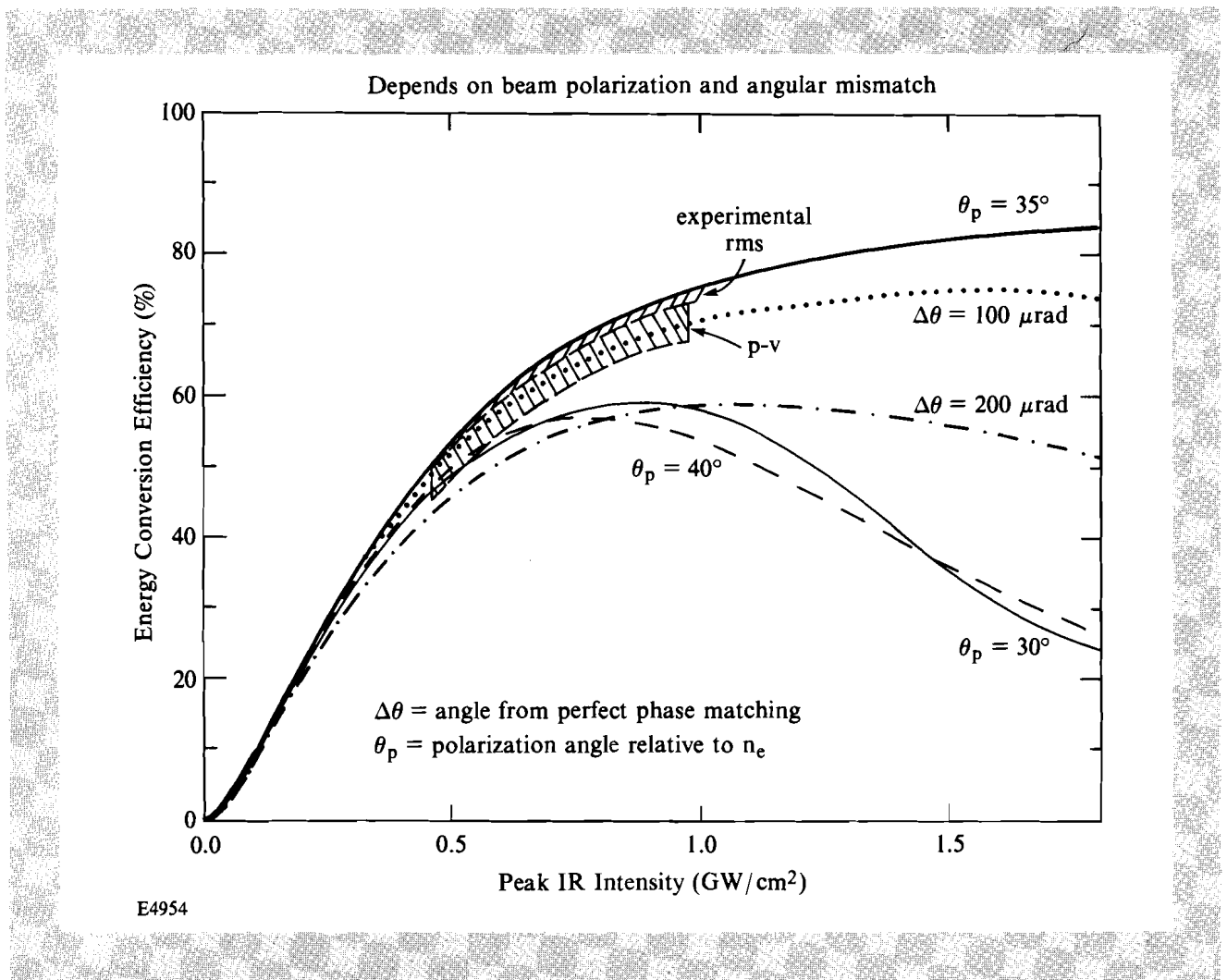
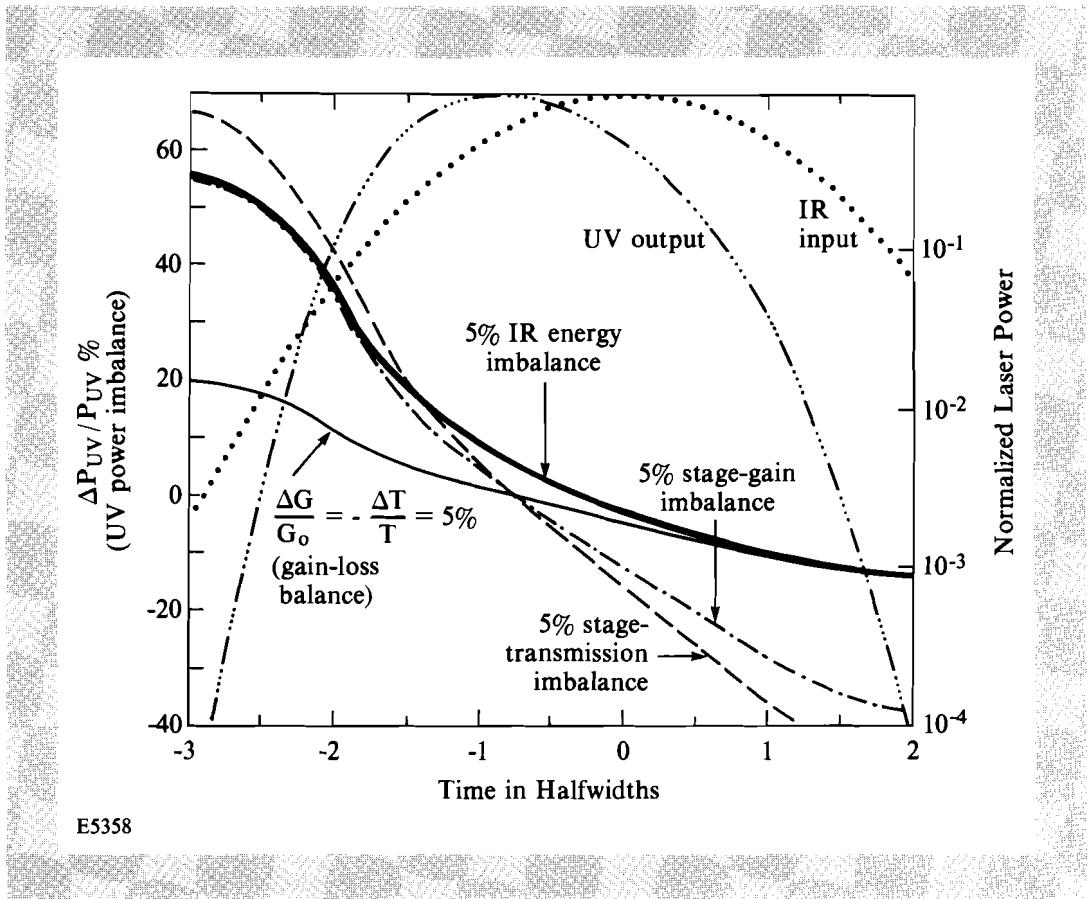


Fig. 41.5

Third-harmonic energy-conversion curves for various angular- and polarization-tuning conditions. Also shown is the range of average 24-beam OMEGA conversion performance (narrow cross-hatched band labeled "experimental rms") and the maximum deviation from perfect tuning (wide cross-hatched band labeled "p-v") taken from over 70 on-target laser system shots.

imbalance in the third harmonic than at the fundamental laser wavelength (compare Figs. 41.4 and 41.6). Balancing gains and losses in the individual amplification stages reduces these effects to manageable levels, as observed for the IR in Fig. 41.4.

In Fig. 41.7 we have summarized the effects of power balance as a result of energy imbalance, gain imbalance, and loss imbalance at 10^{-3} of the peak of the third-harmonic output. If we postulate a maximum-permissible power imbalance of, for example, 20% at any time between any two beams, then we can use Fig. 41.7 to estimate the tolerances on energy balance to be $\leq 2.5\%$, while 6% differences in losses or gains per stage could be acceptable provided they are compensated for, giving equal small-signal gain per stage in the two beamlines. Since these calculations assume that all gains or losses



E5358

Fig. 41.6

Temporal dependence of the UV power balance between two beams of the OMEGA Upgrade at 60-kJ nominal IR output. The heavy solid line is the power balance due to a 5% IR output-energy imbalance; the dashed and dashed-dotted lines are due to 5% transmission (loss) and gain imbalance per stage at perfect IR output-energy balance; and the light solid line corresponds to 5% compensated gains and losses per stage and equal-output beam energies ($\Delta G/G_0 = -\Delta T/T = 5\%$).

per stage of one beam would be increased (or decreased), these results certainly represent a somewhat pessimistic view. On the other hand, achieving even 10% variation in small-signal gains among the equivalent amplification stages of different beamlines represents a challenge in real lasers.

Conclusions

High-compression inertial fusion targets demand a high degree of power balance for all the beams incident on the target. Power balance implies equal pulse shapes and energies in all the beams, placing severe conditions on all nonlinear elements of the laser system such as amplifiers and harmonic frequency converters. We have shown that energy-balance requirements become demanding ($\leq 2\%$ between any two beams) if power balance in the third harmonic output is to stay below $\approx 20\%$ between that pair of beams at any time during the pulse. This condition was derived for laser systems whose beamlines are all identical. If equivalent amplification stages in

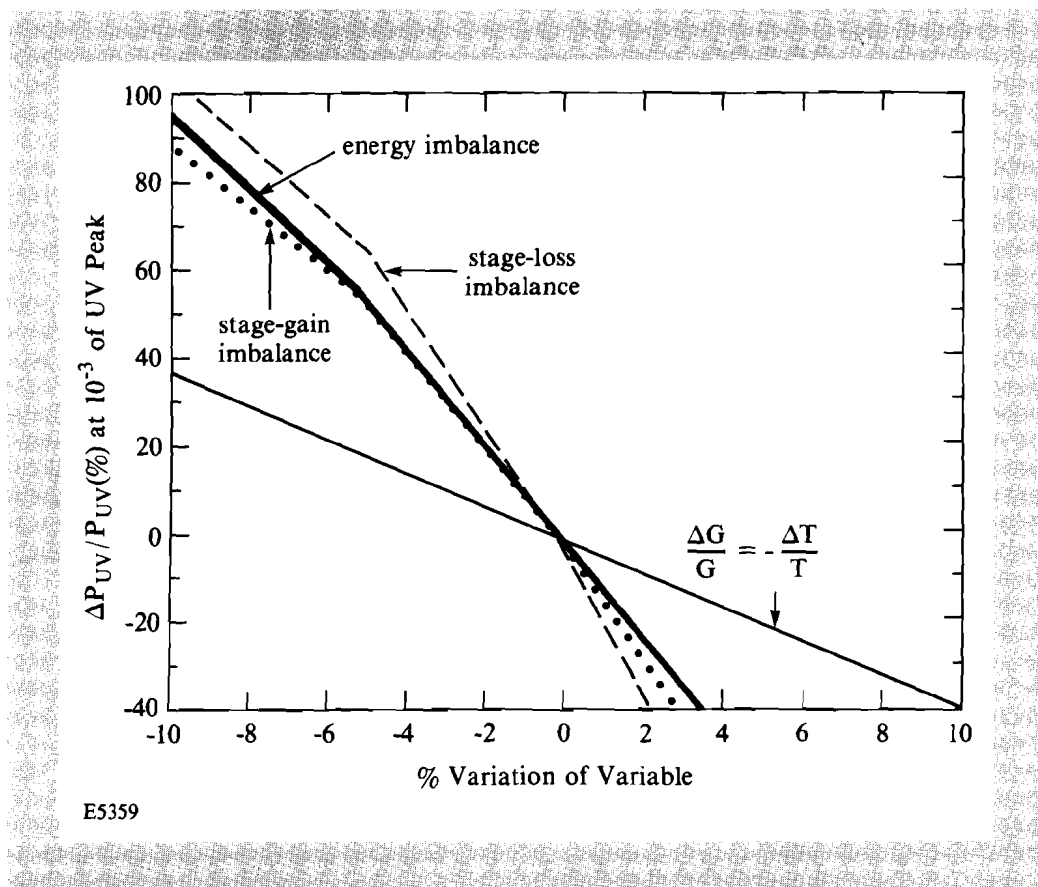


Fig. 41.7

UV power imbalance between two OMEGA Upgrade beamlines at early time when the power has reached 10^{-3} of its peak. The heavy line corresponds to energy imbalance but otherwise identical beams; the other lines correspond to perfect energy balance but different gain or loss imbalance (dotted and dashed curves) and compensated gains and losses per stage ($\Delta G/G = -\Delta T/T$, light solid line).

different beamlines differ in their gains or losses, a very pronounced power imbalance may result even in the presence of perfect energy balance. This detrimental effect is mitigated by balancing the gains and losses in equivalent amplification stages to yield the same net small-signal gain. All these power-balance problems are most noticeable in the early part of the laser pulse rather than near its peak.

In summary, power-balance considerations must form an integral part of any modern design for a laser-fusion facility, and they may significantly impact the staging of the laser system and its efficiency.

ACKNOWLEDGMENT

This work was supported by the U.S. Department of Energy Division of Inertial Fusion under agreement No. DE-FC03-85DP40200 and by the Laser Fusion Feasibility Project at the Laboratory for Laser Energetics, which has the following sponsors: Empire State Electric Energy Research Corporation, New York State Energy Research and Development Authority, Ontario Hydro, and the University of Rochester.

REFERENCES

1. LLE 1989 Annual Report, p. 2 [or LLE Review **37**, 2 (1989)].
2. B. Badger *et al.*, LLE Internal Report #152 (1984); S. Skupsky and K. Lee, *J. Appl. Phys.* **54**, 3662 (1983).
3. S. Skupsky, R. W. Short, T. Kessler, R. S. Craxton, S. Letzring, and J. M. Soures, *J. Appl. Phys.* **66**, 3456 (1989); LLE Review **33**, 1 (1987).

4. F. J. Marshall, S. A. Letzring, C. P. Verdon, S. Skupsky, R. L. Keck, J. P. Knauer, R. L. Kremens, D. K. Bradley, T. Kessler, J. Delettrez, H. Kim, J. M. Soures, and R. L. McCrory, *Phys. Rev. A* **40**, 2547 (1989); R. L. McCrory, J. M. Soures, C. Verdon, M. Richardson, P. Audebert, D. Bradley, J. Delettrez, L. Goldman, R. Hutchison, S. Jacobs, P. Jaanimagi, R. Keck, H. Kim, T. Kessler, J. Knauer, T. Kremens, S. Letzring, F. Marshall, P. McKenty, W. Seka, S. Skupsky, and B. Yaakobi, *Laser Interaction and Related Plasma Phenomena*, Vol. 8, edited by H. Hora and G. H. Miley (Plenum Press, New York and London, 1988), p. 483.
5. J. Bunkenberg, J. Boles, D. C. Brown, J. Eastman, J. Hoose, R. Hopkins, L. Iwan, S. D. Jacobs, J. H. Kelly, S. Kumpan, S. Letzring, D. Lonobile, L. D. Lund, G. Mourou, S. Reformat, W. Seka, J. M. Soures, and K. Walsh, *IEEE J. Quantum Electron.* **QE-17**, 1620 (1981).
6. R. S. Craxton, *Opt. Commun.* **34**, 474 (1980); W. Seka, S. D. Jacobs, J. E. Rizzo, R. Boni, and R. S. Craxton, *Opt. Commun.* **34**, 469 (1980).
7. W. Seka, J. M. Soures, S. D. Jacobs, L. D. Lund, and R. S. Craxton, *IEEE J. Quantum Electron.* **QE-17**, 1689 (1981); J. M. Soures, R. L. McCrory, K. A. Cerqua, R. S. Craxton, R. Hutchison, S. D. Jacobs, T. Kessler, J. Kelly, G. Mourou, W. Seka, and D. Strickland, *Laser Research and Development in the Northeast* (SPIE, Bellingham, WA, 1987), Vol. 709, p. 74.
8. A. E. Siegman, *LASERS*, Chap. 10 (University Science Books, Mill Valley, CA, 1986), p. 362.
9. J. B. Trenholme and K. R. Manes, Lawrence Livermore National Laboratory Report UCRL-51413 (1972); Lawrence Livermore National Laboratory Report UCRL-52868 (1980).
10. W. Friedman, W. Seka, and J. M. Soures, *Opt. Commun.* **25**, 103 (1978).
11. J. T. Hunt and D. R. Speck, *Opt. Eng.* **28**, 461 (1989).
12. L. M. Frantz and J. S. Nodvik, *J. Appl. Phys.* **14**, 2346 (1975).
13. W. E. Martin and D. Milam, *IEEE J. Quantum Electron.* **QE-18**, 1155 (1982).
14. K. Nishihara and S. Nakai, to appear in *Laser Interaction and Related Plasma Phenomena*, edited by H. Hora and G. H. Miley (Plenum Press, New York and London, 1990).
15. J. P. Knauer, R. L. McCrory, J. M. Soures, C. P. Verdon, F. J. Marshall, S. A. Letzring, S. Skupsky, R. L. Kremens, H. Kim, R. Short, T. Kessler, R. S. Craxton, J. Delettrez, R. L. Keck, and D. K. Bradley, to appear in *Laser Interaction and Related Plasma Phenomena*, edited by H. Hora and G. H. Miley (Plenum Press, New York and London, 1990).
16. LLE Review **37**, 16 (1988).